Geophysical Research Letters®

RESEARCH LETTER
10.1029/2021GL094926

Special Section:
The Exceptional Arctic Polar Vortex in 2019/2020: Causes and Consequences

Upper Stratosphere-Mesosphere-Lower Thermosphere Perturbations During the Formation of the Arctic Polar Night Jet in 2019–2020

Renata Lukianova[1,2], Alexander Kozlovsky[3], and Mark Lester[4]

[1]Space Research Institute RAS, Moscow, Russia, [2]Institute of Earth Science, Saint-Petersburg State University, Saint-Petersburg, Russia, [3]Sodankylä Geophysical Observatory, Sodankylä, Finland, [4]Department of Physics and Astronomy, University of Leicester, Leicester, UK

Key Points:

- During the formation of the stratospheric polar vortex, the upper-middle atmosphere is unstable
- Zonal winds amplifications and descending, alternating north/southward flow occur in the stratosphere and mesosphere-lower thermosphere
- Transient warming in the upper stratosphere and cooling above, as well as mesospheric thermal inversions are observed

Correspondence to:
R. Lukianova,
renata@aari.ru

Citation:
Lukianova, R., Kozlovsky, A., & Lester, M. (2021). Upper stratosphere-mesosphere-lower thermosphere perturbations during the formation of the Arctic polar night jet in 2019–2020. *Geophysical Research Letters*, *48*, e2021GL094926. https://doi.org/10.1029/2021GL094926

Received 18 JUN 2021
Accepted 20 SEP 2021

Abstract Thermal and dynamic perturbations in the polar upper stratospheric/mesosphere-lower thermosphere in the Arctic winter of 2019–2020 as measured by a meteor radar at 67°N, Aura Microwave Limb Sounder and reanalysis are presented. The most severe disturbances occur from late December to mid-January, while the rest of the winter is relatively stable. Mesospheric winds are dominated by several impulsive increases in the zonal component, an abrupt descent of the wind core and alternating north- and south-ward flow with a period of half a month. Reduced temperature at 90 km height accompanied by thermal inversions is observed in association with upper stratosphere/lower mesosphere warming in the eastern hemisphere. The warming trend is interrupted by a strong cooling in the entire stratosphere-mesosphere. The upper middle atmosphere appears considerably stratified. High "walls" surround the vortex that is favorable for its stability.

Plain Language Summary If the stratospheric polar vortex is strong, it serves as a stable background for the overlying atmosphere, which remains undisturbed because waves and heat do not penetrate there from below. In the Arctic winter of 2019–2020, although the vortex is evolved into such a configuration and became exceptionally strong in the late winter, during its initial formation, dramatic disturbances occurred in the upper stratosphere and mesosphere. Impulsive strengthening and descending of the zonal winds, shears, alternating north- and south-ward flows, transient upper stratospheric warming and mesospheric cooling, persistent thermal inversions, observed in the first half of the winter, likely indicate a certain degree of decoupling of the atmospheric layers and the role of the high-altitude atmosphere in the intensification and splitting of the vortex.

1. Introduction

In the Northern Hemisphere winter of 2019/2020, a very strong, cold and persistent westerly circulation occurred in the high-latitude stratosphere. Unlike ordinary Arctic winters during which stratospheric warmings (minor or major)are relatively common, in this particular winter the polar vortex was less disturbed or weakened by upward propagating planetary waves from the troposphere. It has been shown that a reflective configuration in the upper stratospheric circulation was formed when the upward propagating tropospheric waves did not exhibit much breaking in the stratosphere. Two-way coupling between the troposphere and cold stratosphere resulted in the strong positive phase of the Arctic Oscillation and the deepest ever observed spring-time ozone depletion in the Arctic (Lawrence et al., 2020).

Perturbations in the stratosphere and troposphere as well as the dynamical coupling of these atmospheric layers during the unusual winter of 2019/2020 became the subject of active research as can be seen from the large number of articles published within the framework of a special collection. Less attention is paid to the upper atmosphere, which can also be involved. The mesosphere-lower thermosphere (MLT) is located at 60–100 km altitude and coupled vertically to the stratosphere by radiative, dynamical and chemical processes. The phase of thermal regimes in the high-latitude stratosphere and mesosphere is opposite. While the winter stratosphere is cold due to reduced radiative input, the MLT is warm because of downwelling induced by the high-altitude pole-to-pole circulation. The transient perturbations associated with a major sudden stratospheric warming (SSW) are identified as a mesospheric cooling and wind reversals (Cho et al., 2004; Hoffmann et al., 2007; Labitzke, 1972; Liu & Roble, 2002; Lukianova et al., 2015; Matsuno, 1971;

Siskind et al., 2005; Walterscheid et al., 2000). A SSW is maintained by atmospheric waves of various scales that force the middle atmosphere from below. During the non-SSW winters, the high-latitude MLT is commonly considered stable. If an undisturbed polar jet prevails in the underlying stratosphere, the MLT is dominated by the eastward/poleward wind with a speed up to several tens of meters per second and an average temperature of ∼180 K (Lukianova et al., 2018; Portnyagin et al., 2004).

In 2019/2020, the stratospheric polar vortex greatly exceeded the ordinary level of intensity. The question arises whether the region above the stratopause could also be involved in this climatic extreme. It should be noted that the current period of low solar activity is favorable for a clearer identification of intra-atmospheric variability at higher altitudes. In this letter we explore the structure and evolution of the thermodynamic fields in the stratosphere-mesosphere during the winter of 2019/2020 combining the global and local observations.

2. Data

We use data from several sources, namely, mesospheric winds from the meteor radar (MR) operated by the Sodankyla Geophysical Observatory (SGO, 67°22′N, 26°38′E), the temperature data from the Earth Observing System Microwave Limb Sounder (MLS) on board the Aura satellite (Waters et al., 2006), and the NASA Modern-Era Retrospective analysis for Research and Applications (MERRA-2) reanalysis (Gelaro et al., 2017).

The primary application of MR is to measure neutral wind and temperature in the MLT. The physical basis behind this facility is that meteoroids entering the Earth's atmosphere form ionized trails at heights between 80 and 100 km, which reflect radio waves. The SGO MR is a commercially produced SKiYMET all-sky interferometric radar with standardized software for data processing. It consists of one antenna transmitting spherical VHF waves at 36.9 MHz and five antennas receiving reflections from the meteor echoes. The MR observations of the position and radial velocity of several thousand trails per day allow determining the zonal and meridional components of the neutral wind at ∼3 km height intervals from 82 to 98 km altitude with 1 h time resolution. The daily temperature data at the height of maximum meteor detection at ∼90 km are calculated from the decay time of meteor trails (Hocking, 1999). In the winter of 2019/2020, SGO MR provided measurements near the edge of the stratospheric polar vortex, where the strongest anomaly of geopotential height (GPH) at a pressure level of 10 hPa was about $-5{\cdot}10^4$ m.

The Aura satellite has a Sun-synchronous, near polar orbit at ∼700 km altitude with 13 orbits per day. The local times when passing the SGO MR location are about 3 and 12 hr. The MLS sounder on board the satellite observes the faint microwave emissions from the Earth limb viewing forward along the flight direction. Above the stratopause, the vertical resolution is approximately 8 km, the horizontal resolution is ∼170 km along the orbital track and 12 km cross track. Temperatures at 54 levels up to 0.0001 hPa are available with 1–2.5 K precision. The longitudinal separation of MLS measurements is 10–20°. The MLS data Level 2, version 4 (Livesey et al., 2020) are used to obtain the vertical temperature profiles.

Climate reanalysis data from MERRA-2 beginning in 1980 to the present are used to construct the stratospheric winds in December 2019–February 2020. The 3-hr temporal and 0.5° × 0.625° spatial resolution data up to 0.1 hPa are available via a web-based system NASA Geospatial Interactive Online Visualization And aNalysis Infrastructure (GIOVANNI) developed by the Goddard Earth Sciences Data and Information Services Center (GES DISC).

3. Winds

3.1. Stratospheric Zonal Winds

The polar vortex is represented by a circumpolar westerly flow, cold temperatures and small GPH in the center. Figure 1 depicts the daily MERRA-2 stratospheric zonal winds at the pressure levels from 100 to 0.1 hPa in December–February. Figure 1a shows the vertical cross-section of the circumpolar flow averaged over 60°–80°N. Figure 1b shows a portion of the polar vortex above the SGO MR location. Here, winds are averaged over 65°–70°N and 0°–50°E, that is, over the area extended to approximately 2° north and south and to 25° east and west from the central point. Both the global vortex and its local part are relatively

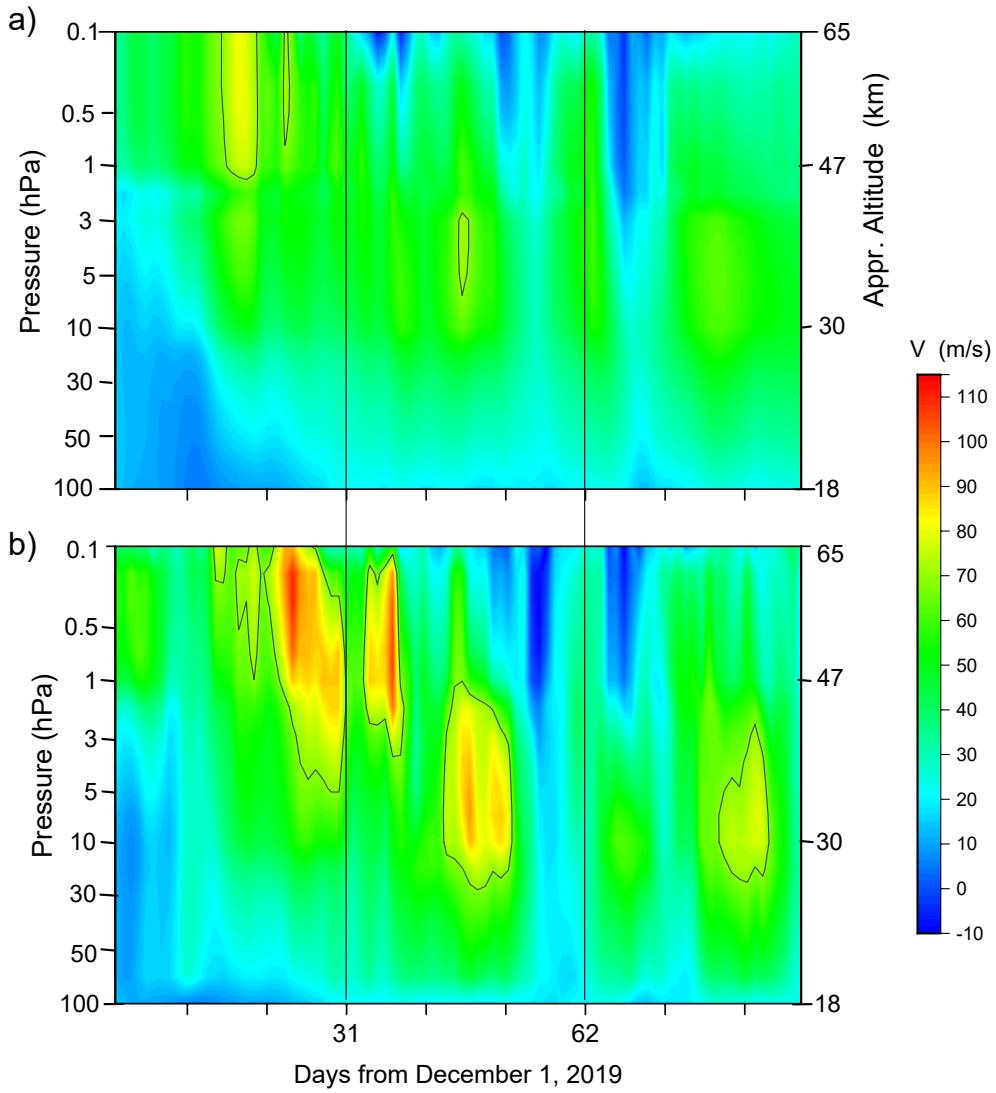

Figure 1. Vertical cross-section of the daily Modern-Era Retrospective analysis for Research and Applications-2 zonal mean zonal winds (positive eastward) averaged within (a) 60°–80°N, all longitudes and (b) 65°–70°N, 0°–50°E in the height interval of 100–0.1 hPa in December 2019–February 2020. Black lines mark the contour of 70 m/s.

coherent, although the latter has considerably higher velocity and variability. Eastward winds start to accelerate at the highest altitudes in mid-December. The peak value of the zonal mean zonal wind rapidly increase up to ~80 m/s (Figure 1a), while the local velocities reach 110 m/s (Figure 1b). To highlight the strongest winds, areas where the speed exceeds 70 m/s (an arbitrary value) are highlighted with black line. The fact that the local wind is stronger than the zonal mean zonal wind likely indicates a distortion of the vortex and its displacement from the pole toward Northern Europe. From mid-December to mid-January, the local part is dominated by several pulses of accelerating winds, in which shorter-period high-amplitude oscillations are embedded.

Another notable feature evident from Figure 1, especially in a regional scale, is downwelling in mid-January, when the wind core drops sharply from 0.2 to 5 hPa (approx. 60 and 35 km altitude). As a result, in early winter, the upper stratospheric winds are much stronger than those in the middle/lower stratosphere, while during the rest of the winter, the upper winds are weaker than the lower ones. Throughout the stratosphere, the flow is eastward, but the difference between the lower and upper winds forms a stratification reminiscent of wind shear. Assuming the largest difference between velocities above and below the pressure

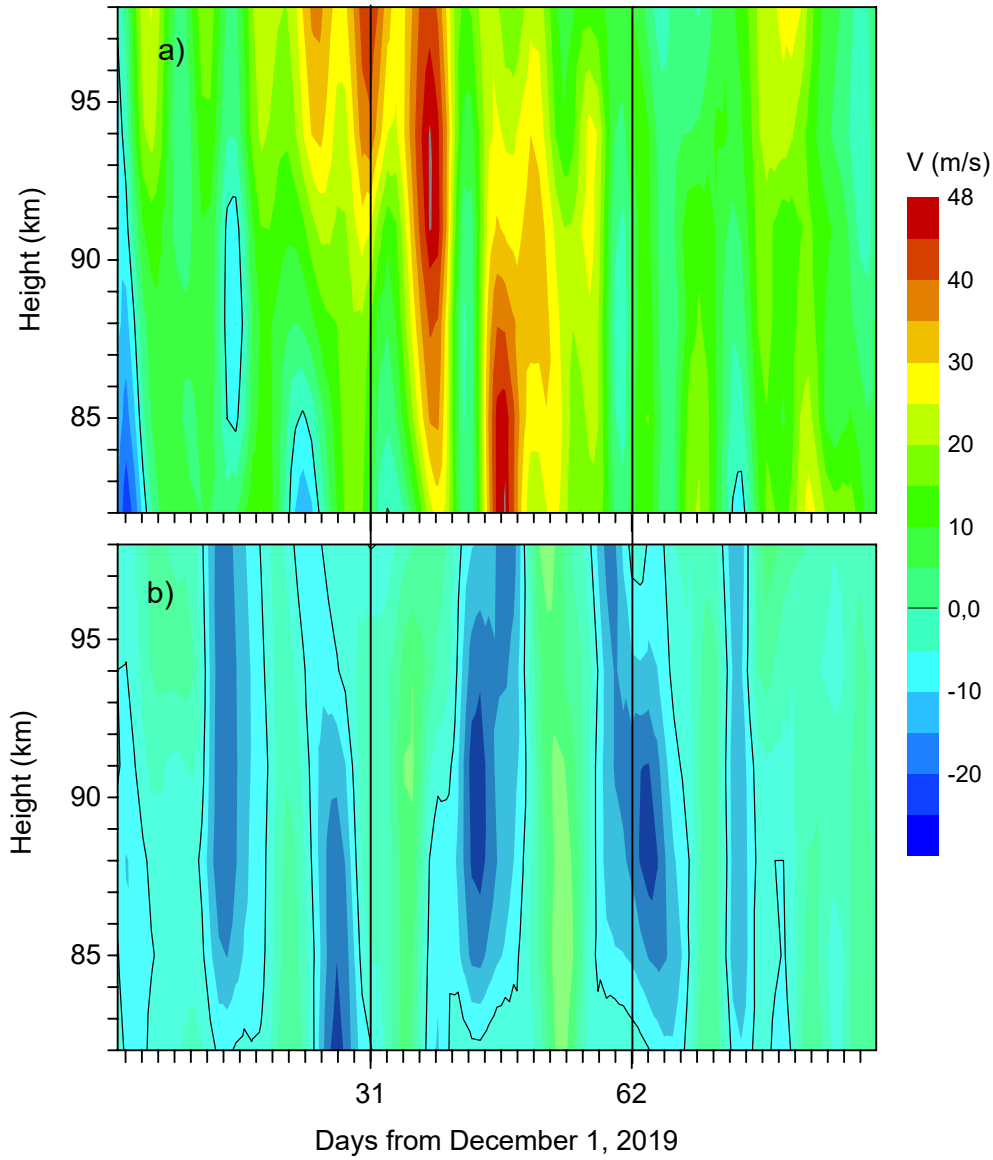

Figure 2. The Sodankyla Geophysical Observatory meteor radar (a) zonal and (b) meridional winds in December–February (positive east- and north-ward). Black lines mark the zero winds.

level of 2 hPa (~47 km) as 50 m/s and the thickness of the corresponding layer as 5 km, the vertical shear is estimated as 10 m/s/km.

3.2. Mesospheric Winds

Dynamic perturbations in the stratosphere are often extended to MLT heights. In fact, at these altitudes, meteor radar is the only instrument capable of regularly measuring wind. An additional advantage relates to the enhanced stratospheric winds over the SGO over the mean circumpolar flow, suggesting that the SGO MR is located in the vicinity of particularly large disturbances. Changes in MLT circulation in December-February are shown in Figure 2, which presents the SGO MR zonal (Figure 2a) and meridional (Figure 2b) winds at heights 82–98 km. Apparent in Figure 2a are wave-like structures which consisting of four strong short-lived (several days long) pulses, up to 50 m/s, propagating downward. As the velocity changes with height, several vertical shear structures are formed. The largest occur in the first and second decades of January, when the wind core is observed, respectively, above and below the mesopause at ~88 km. In

the meridional winds (Figure 2b), systematic north-southward fluctuations prevail, at which the southward flow strengthens up to 30 m/s. The Fourier decomposition gives a broad peak at a planetary wave period of 10–16 days (not shown).

4. Stratospheric and Mesospheric Temperatures

It is known that mesospheric and stratospheric temperatures are significantly anticorrelated (e.g., Siskind et al., 2005). The annual pattern from the SGO MR temperature related to an altitude of 90 km consists of warm winters (~180 K) and cold summers (~120 K). The daily values are more perturbed in winter and may suddenly drop down to 150 K during a SSW (Lukianova et al., 2015). Recently, it was noticed that the temperature during the Geminids meteor shower in mid-December is underestimated by the routine MR calculations. This is because of specific properties of the meteoroids belonging to the shower. The same, albeit much weaker, effect was found in early January during the Quadrantids (Kozlovsky et al., 2016). Keeping these limitations in mind we will estimate the temperature perturbations in the months of interest using the SGO MR and the Aura MLS instrument.

Figure 3 shows the daily temperatures measured locally. The SGO MR temperatures at 90 km height are depicted in Figure 3a. Several days during the Geminids are excluded. The main feature noteworthy in Figure 3a is a cooling that begins in late December, peaks in early January (with a negative excursion down to 135 K on January 4), and saturates in mid-January. Figure 3b depicts the evolution of the MLS temperatures for the SGO MR location. The analysis includes measurements from the 67.5°N and 16–36°E (~10° east and west of SGO longitude) and temperatures from longitude-spaced tracks are linearly interpolated and centered at 26°E. An episode of the mesospheric cooling at 0.01 hPa is clearly seen in the MLS data. It is formed above a peak of warming at 0.1–2 hPa, which begins in late December. Later, in early January, the temperatures increase by about 50K (up to 290 K) comparing with those in mid-December. This thermal structure is known as the upper stratosphere/lower mesosphere (USLM) disturbance (Greer et al., 2013). The observed mid-January USLM event lasts more than two weeks and is abruptly interrupted by a cooling (a drop to 220 K) of the entire stratosphere, accompanied by a warming of the mesosphere. During the rest of the winter the stratospheric temperature is relatively stable (~260 K in the stratopause).

The temperature fields from MERRA indicate that the USLM warming is associated with planetary wave 1 in the upper stratosphere. Figure 4 is a Hovmöller "time-longitude" plot of temperatures at 1 hPa (~47 km), averaged over 60–90°N. The diagram shows that in the first decade of January there is an increase in the zonal asymmetry of wave 1 and USLM warming in the eastern hemisphere (0–100°E). It appears the SGO MR observations are carried out in the immediate vicinity of the ridge of wave 1. Note, with a growth of wave 1, the polar vortex may displace from the pole, as evidenced by a stronger local stratospheric zonal wind, while the zonal mean zonal wind is moderate, as shown in Figure 1.

Figure 5 shows the evolution of the vertical profile of MLS temperature at the SGO location at different stages of the winter thermal regime. Three distinctive shapes with respect to the stratopause height and mesospheric inversion layer can be found. In December, the stratopause of ~265 K is at its maximum altitude (65 km), the mesospheric thermal inversion is marginal; in early January the stratopause drops to 47 km, the mesosphere becomes cooler, and the inversion deepens by ~25 K, from 210 to 185 K, (for the period, the climatological profile is also shown); in the rest of the winter, the stratopause is stabilized at 47 km and the mesospheric temperature profiles show a monotonic cooling with height.

5. Discussion

The observations presented above reveal dramatic meteorological disturbances which affect a wide range of altitudes in the high-latitude winter atmosphere. The USLM/MLT heights are disturbed by a transient warming/cooling dipole, planetary waves, impulsive descending of the zonal winds and thermal inversions. These disturbances occur in the first half of winter when the stratospheric polar vortex is just establishing. Lawrence et al. (2020) pointed out that the vortex was extraordinarily strong during the Northern winter of 2019/2020 due to unusually weak tropospheric wave activity and wave reflection events in the polar upper stratosphere. The reflective configuration was formed when a "split" jet structure emerged, that is, there are

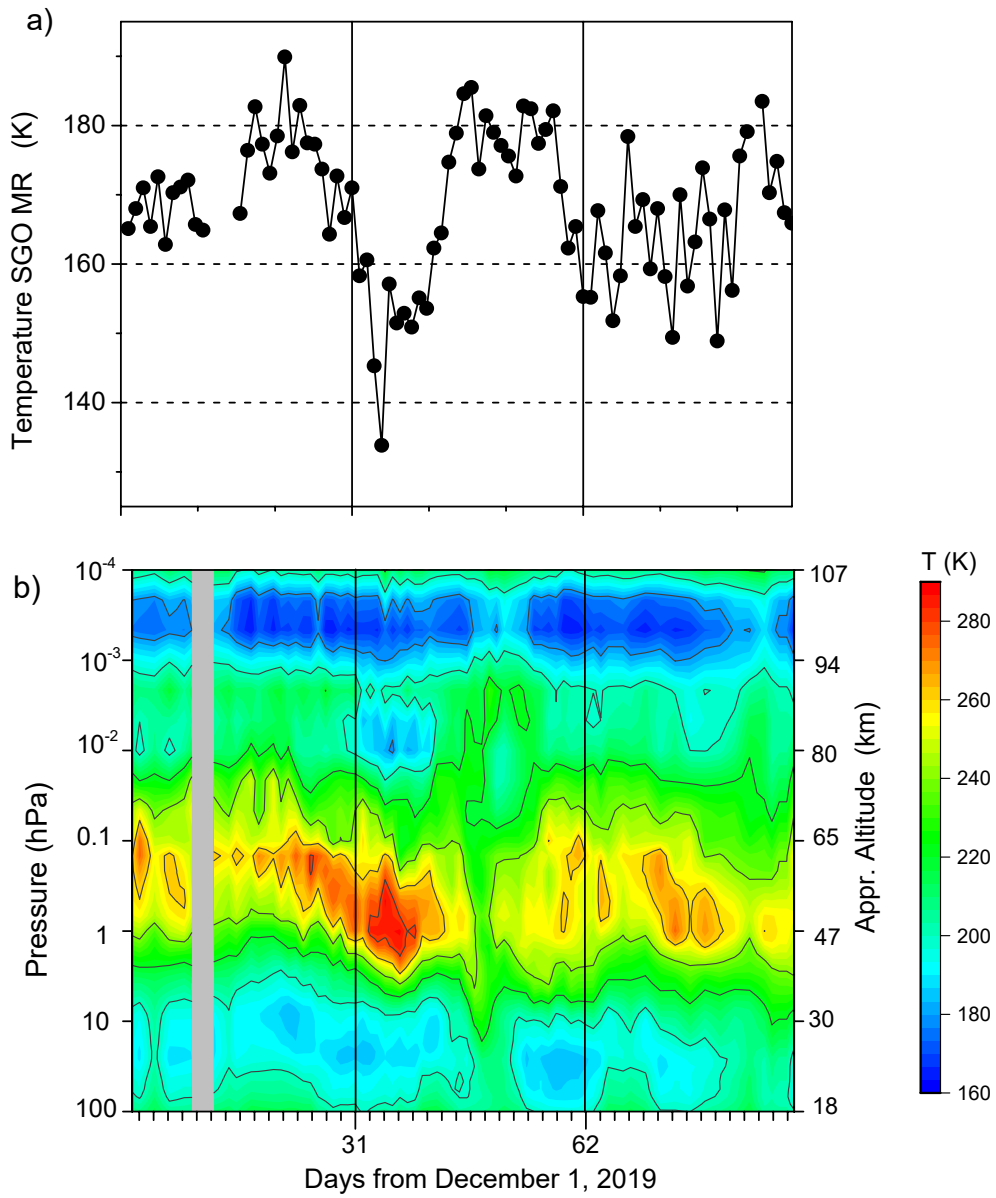

Figure 3. (a) The Sodankyla Geophysical Observatory (SGO) meteor radar (MR) temperatures at 90 km; (b) the vertical cross-section of the Microwave Limb Sounder temperatures over SGO in December–February.

two zonal wind maxima, the subtropical jet in the USLM and the polar jet at high latitudes in the lower/upper stratosphere which was shifted poleward under wave driving in early January. Downward reflection of waves resulted in strengthening and stabilization of the vortex in the lower stratosphere in the second half of the winter season.

Our results confirm that the upper stratosphere is disturbed in such a way that strong zonal winds occur in late December and rapidly descend by about 25 km in mid-January. Radar observations of the MLT show successive pulses of the eastward winds. The wind core moves downward, producing wind shears, with the first occurring at an altitude of ~94 km or higher, and the next occurring at lower altitudes. The observed shears of up to 10 m/s/km are the largest ever observed by SGO MR since its deployment in 2008 but are considerably weaker than those what could be sustained before the mesosphere undergoes dynamic instability (several tens of m/s/km) according to the estimate by Liu (2017).

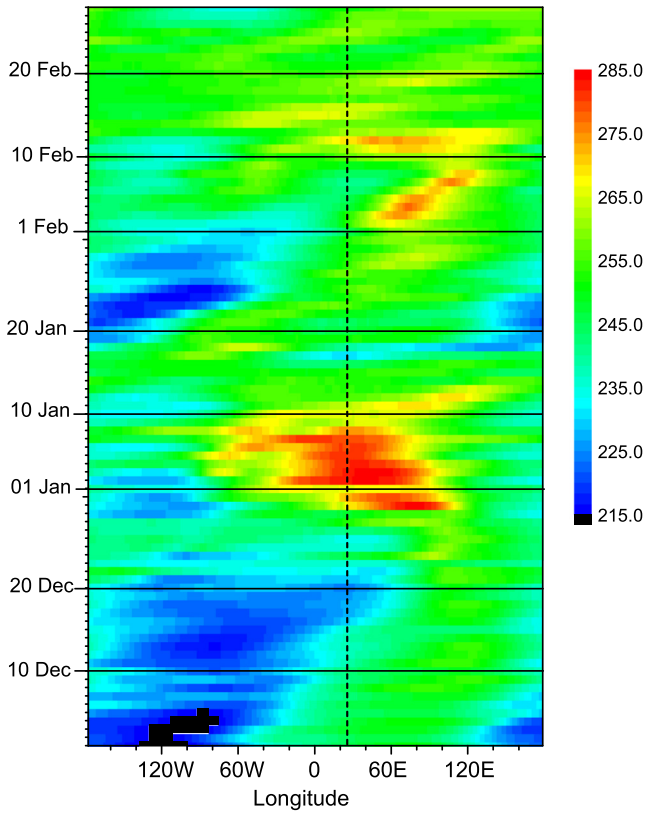

Figure 4. Hovmöller "time-longitude" plot of temperatures at 1 hPa, 60–90°N. Vertical dotted line marks the longitude of the Sodankyla Geophysical Observatory meteor radar.

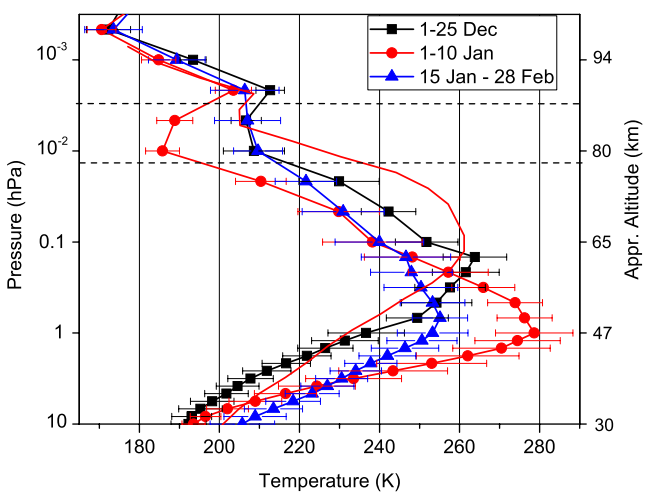

Figure 5. The Microwave Limb Sounder temperature vertical profiles over Sodankyla Geophysical Observatory for the three periods of the 2019/2020 winter (lines with symbols) and the climatological profile for the period of January 1–10 (red line without symbols). The dashed lines show the inversion layer.

The signature of descending winds may also be indicative of a wave front which is somewhat tilted. To determine the true direction, analysis of multi-radar observations is required. It is nevertheless obvious that in December–January the impulsive enhancement of the westerlies, accompanied by an abrupt descending of the wind core, occupy a wide range of heights in the stratosphere and MLT. We speculate that the "split" jet structure, which is formed in January and consists of a high-latitude jet in the stratosphere and a subtropical jet in the USLM, as shown by Lawrence et al. (2020), expands up to MLT heights, so that the "walls" surrounding the polar vortex is very high, that may create favorable conditions for the strong vortex. The MLT is also dominated by half-a-month waveforms, which are manifested in the systematic alternation of poleward (weaker) and equatorward (stronger) winds. Normally the SGO MR doesn't observe waves of this intensity and their appearance may be due to the strong polar vortex.

Although the vortex evolves into strong and stable configuration, during the period of its formation (December–mid-January) the entire middle atmosphere is far from stability. A clear tendency to the warm stratosphere takes place, since USLM event is reminiscent of a SSW but in this case confined to polar latitudes and upward of the upper stratosphere. The vertical profiles of temperatures shows anomalously warm and low stratopause, cooling of the mesosphere and inversion layer below the mesopause. The magnitude of the inversions is highly correlated with planetary wave amplitude, so that large inversions usually develop during episodes of planetary wave amplification (Sassi et al., 2002). Greer et al. (2013) have shown that USLM disturbances often occur prior to the onset of SSWs. During USLM conditions, the polar vortex is distorted and displaced from the pole toward the Greenwich Meridian. It is these features that are observed in the winter of 2019–2020. However, in mid-January, the warming does not evolve into a SSW but is abruptly interrupted by a rapid cooling of the entire stratospheric layer. This occurred in association with a burst of the periodic zonal wind accelerations and in conjunction with a rapid descending of the wind core in a wide range of altitudes.

We explored the structure of USLM and MLT in the whole winter of 2019–2020. However, it appears that the great majority of dramatic disturbances occur from December to mid-January, while the rest of the winter is relatively stable. During this initial period the conditions favorable for the formation of extreme polar vortex are created. The high-latitude USLM/MLT is considerably stratified, the atmospheric layers seem to be decoupled, so the "forcing from below" is relatively weak. Rather, the polar vortex is amplified by being confined by the low-latitude jet in the USLM which is formed during a "split" event as revealed by Lawrence et al. (2020). The altitudes of this interaction extend up to 100 km and even higher.

6. Conclusion

Combining datasets provided by Aura MLS, meteor radar and reanalysis, we present observational evidence for unusual changes in the thermal and dynamic regime in the USLM/MLT during the winter of 2019–2020. A great majority of dramatic disturbances occur from late December to mid-January, while the rest of the winter is relatively stable. The

Sodankyla meteor radar (67°N, 26°E) located under the ridge of wave 1, observes several successive pulses of the eastward wind at high velocities up to 50 m/s. The wind core first appears at high altitudes and then descends abruptly, resulting in wind shears and stratification of zonal flow over a wide range of heights in USLM/MLT. The meridional component of the MLT winds is dominated by the alternating north- and southward flows with a half-a-month period. Temperatures at MLT heights decrease due to USLM warming that begins in late December. In mid-January, this structure is interrupted by an abrupt cooling throughout the entire middle atmosphere. During the initial formation of a strong stratospheric polar vortex the MLT and USLM seem largely decoupled relative to the forcing from below. Rather, high and strong "wall" surrounding the vortex is formed, likely in association with high-altitude disturbances in the lower latitudes.

Conflict of Interest

The authors declare no conflicts of interest relevant to this study.

Data Availability Statement

NASA MERRA-2 data are available from NASA's GES DISC web-based system Giovanni (https://giovanni.gsfc.nasa.gov/giovanni/); AURA MLS temperature data are available from the Open-source Project for a Network Data Access Protocol (OPeNDAP) (https://acdisc.gesdisc.eosdis.nasa.gov/opendap/hyrax/HDF-EOS5/Aura_MLS_Level2/ML2T.004); the data from the Sodankyla Geophysical Observatory Meteor radar are available at https://www.sgo.fi/Data/observations.php.

Acknowledgments
R. Lukianova acknowledges support from the Academy of Finland via grant 339849. M. Lester acknowledges support from STFC grant ST/S000429/1.

References

Cho, Y.-M., Shepherd, G. G., Won, Y.-I., Sargoytchev, S., Brown, S., & Solheim, B. (2004). MLT cooling during stratospheric warming events. *Geophysical Research Letters*, *31*, L10104. https://doi.org/10.1029/2004GL019552

Gelaro, R., McCarty, W., Suárez, M. J., Todling, R., Molod, A., et al. (2017). The modern-era retrospective analysis for research and applications, version-2 (MERRA-2). *Journal of Climate*, *30*, 5419–5454. https://doi.org/10.1175/JCLI-D-16-0758.1

Greer, K. R., Thayer, J. P., & Harvey, V. L. (2013). A climatology of polar winter stratopause warmings and associated planetary wave breaking. *Journal of Geophysical Research: Atmosphere*, *118*, 4168–4180. https://doi.org/10.1002//jgrd.50289

Hocking, W. K. (1999). Temperatures using radar-meteor decay times. *Geophysical Research Letters*, *26*(21), 3297–3300. https://doi.org/10.1029/1999GL003618

Hoffmann, P., Singer, W., Keuer, D., Hocking, W. K., Kunzec, M., & Murayama, Y. (2007). Latitudinal and longitudinal variability of mesospheric winds and temperatures during stratospheric warming events. *Journal of Atmospheric and Solar-Terrestrial Physics*, *69*(17–18), 2355–2366. https://doi.org/10.1016/j.jastp.2007.06.010

Kozlovsky, A., Lukianova, R., Shalimov, S., & Lester, M. (2016). Mesospheric temperature estimation from meteor decay times during Geminids meteor shower. *Journal of Geophysical Research: Space Physics*, *121*, 1669–1679. https://doi.org/10.1002/2015JA022222

Labitzke, K. (1972). Temperature changes in the mesosphere and stratosphere connected with circulation changes in winter. *Journal of Atmospheric Science*, *29*, 756–766.

Lawrence, Z. D., Perlwitz, J., Butler, A. H., Manney, G. L., Newman, P. A., et al. (2020). The remarkably strong Arctic stratospheric polar vortex of winter 2020: Links to record-breaking Arctic Oscillation and ozone loss. *Journal of Geophysical Research: Atmospheres*, *125*, e2020JD033271. https://doi.org/10.1029/2020JD033271

Liu, H.-L. (2017). Large wind shears and their implications for diffusion in regions with enhanced static stability: The mesopause and the tropopause. *Journal of Geophysical Research: Atmospheres*, *122*, 9579–9590. https://doi.org/10.1002/2017JD026748

Liu, H.-L., & Roble, R. G. (2002). A study of a self-generated stratospheric sudden warming and its mesospheric-lower thermospheric impacts using the coupled TIMEGCM/CCM3. *Journal of Geophysical Research*, *107*, 4695–4712. https://doi.org/10.1029/2001JD001533

Livesey, N. J., Read, W. G., Wagner, P. A., Froidevaux, L., Lambert, A., Manney, G. L., & Lay, R. R. (2020). *EOS MLS version 4.2× level 2 and 3 data quality and description document: JPL*. Retrieved from https://mls.jpl.nasa.gov/data/v4-2_data_quality_document.pdf

Lukianova, R., Kozlovsky, A., & Lester, M. (2018). Climatology and inter-annual variability of the polar mesospheric winds inferred from the meteor radar observations over Sodankylä (67N, 26E) during solar cycle 24. *Journal of Atmospheric and Solar-Terrestrial Physics*, *171*, 241–249. https://doi.org/10.1016/j.jastp.2017.06.005

Lukianova, R., Kozlovsky, A., Shalimov, S., Ulich, T., & Lester, M. (2015). Thermal and dynamical perturbations in the winter polar mesosphere-lower thermosphere region associated with sudden stratospheric warmings under conditions of low solar activity. *Journal of Geophysical Research: Space Physics*, *120*, 5226–5240. https://doi.org/10.1002/2015JA021269

Matsuno, T. (1971). A dynamical model of the stratospheric sudden warming. *Journal of Atmospheric Science*, *28*, 1479–1494.

Portnyagin, Y., Solovjova, T. V., Makarov, N. A., Merzlyakov, E. G., Manson, A. H., et al. (2004). Monthly mean climatology of the prevailing winds and tides in the Arctic mesosphere/lower thermosphere. *Annales Geophysicae*, *22*, 3395–3410. https://doi.org/10.5194/angeo-22-3395-2004

Sassi, F., Garcia, R. R., Boville, B. A., & Liu, H. (2002). On temperature inversions and the mesospheric surf zone. *Journal of Geophysical Research*, *107*(D19), 4380. https://doi.org/10.1029/2001JD001525

Siskind, D. E., Coy, L., & Espy, P. (2005). Observations of stratospheric warmings and mesospheric coolings by the TIMED SABER instrument. *Geophysical Research Letters*, *32*, L09804. https://doi.org/10.1029/2005GL022399

Walterscheid, R. L., Sivjee, G. G., & Roble, R. G. (2000). Mesospheric and lower thermospheric manifestation of a stratospheric warming eventover Eureka, Canada (80°N). *Geophysical Research Letters*, *27*, 2897–2900. https://doi.org/10.1029/2000GL003768

Waters, J. W., Froidevaux, L., Harwood, R. S., Jarnot, R. F., Pickett, H. M., et al. (2006). The earth observing system microwave limb sounder (EOS MLS) on the Aura satellite. *IEEE Transactions on geosciences and remote sensing*, *44*(5), 1075–1092.